ISSN 1674-1056
http://cpb.iphy.ac.cn
http://iopscience.iop.org/cpb
中国物理 B
Chinese Physics
中国物理
Chinese Physics B

Cavity formation during water entry of heated spheres

Jia-Chuan Li(李佳川), Ying-Jie Wei(魏英杰), Cong Wang(王聪), Wei-Xue Xia(夏维学)

Citation: Chin. Phys. B . 2018, 27(9): 094703. **doi:** 10.1088/1674-1056/27/9/094703

Journal homepage: http://cpb.iphy.ac.cn; http://iopscience.iop.org/cpb

What follows is a list of articles you may be interested in

The influence of surface effects on Frederiks transition in nematic liquid crystal doped with ferroelectric nanoparticles

Erfan Kadivar, Mojtaba Farrokhbin

Chin. Phys. B . 2018, 27(4): 046801. **doi:** 10.1088/1674-1056/27/4/046801

Phase transition and critical behavior ofspin-orbital coupled spinel ZnV_2O_4

Li Wang(王理), Rong-juan Wang(王蓉娟), Yuan-yuan Zhu(朱媛媛), Zhi-hong Lu(卢志红),Rui Xiong(熊锐), Yong Liu(刘雍), Jing Shi(石兢)

Chin. Phys. B . 2016, 25(1): 016802. **doi:** 10.1088/1674-1056/25/1/016802

An effective-field theory study of hexagonal Ising nanowire：Thermal and magnetic properties

Yusuf Kocakaplan, Ersin Kantar

Chin. Phys. B . 2014, 23(4): 046801. **doi:** 10.1088/1674-1056/23/4/046801

Cavity formation during water entry of heated spheres*

Jia-Chuan Li(李佳川), Ying-Jie Wei(魏英杰)†, Cong Wang(王聪), and Wei-Xue Xia(夏维学)

School of Astronautics, Harbin Institute of Technology, Harbin 150001, *China*

(Received 27 February 2018; revised manuscript received 15 May 2018; published online 28 August 2018)

We experimentally study the cavity formation when heated spheres impact onto water at low and high subcooling. The observations present that the formation and appearance of the cavity are affected by the boiling modes and the heat transfer intensity. In the nucleate-boiling regime, a rough cavity can be formed at a rather low impact velocity, while at the same velocity, the cavity formed in the film-boiling regime may have a very smooth interface with a stable vapor layer around the sphere. We discuss the effects of the impact speed, water and sphere temperatures on the stability of the vapor layer. For low subcooled water, the stable vapor layer will be disturbed when increasing the impact velocity, leading to a disturbed cavity. For high subcooled water, the film boiling has a particular boiling model in which the vapor layer around the sphere cannot keep its stability. In this particular film-boiling regime, no cavities can be formed at low impact velocities and only broken cavities can be formed at high impact velocities.

Keywords: water-entry cavity, boiling, vapor layer

PACS: 47.55.dp, 47.54.De, 68.35.Rh **DOI:** 10.1088/1674-1056/27/9/094703

1. Introduction

When a rigid body impacts onto a liquid, complex flow phenomena occur, and a splash and cavity can be formed during the impact. The water-entry problems are directly relevant to aerospace, naval, and military applications.[1–3] The presence of a water-entry cavity has a dramatic influence on the structural characteristics and ballistic stability for weapons such as aerial torpedoes and water-entry missiles. The splash and cavity photographs were firstly captured by Worthington *et al.*[4,5] and Worthington[6] through using single spark photography. They analyzed the effects of impact velocity and liquid density, viscosity, and surface tension on water-entry splash. Since then, extensive experiments have been performed to study the water-entry characteristics of spheres. May[7] investigated the effect of the surface condition of spheres on cavity formation; he found that contaminated spheres can form cavities at much lower impact velocities than clean ones. Aristoff *et al.*[8] conducted water-entry experiments with low-density spheres, and investigated the influence of deceleration on cavity shape. Duez *et al.*,[9] Duclaux *et al.*,[10] and Aristoff *et al.*[11] investigated the wettability effect on the cavity formation and evolution through using hydrophobic spheres.

Theoretical models have been developed to describe the evolution of cavity shape by Duclaux *et al.*[10] and Aristoff *et al.*[11] Duclaux *et al.*[10] derived a cavity evolution expression in the limit where viscous and capillary effects can be ignored. The theoretical solution predicts the pinch-off depth of the cavity in two different regimes. When the cavity evolution is mainly driven by surface tension rather than gravity, the model given by Aristoff *et al.*[11] can be used to obtain an approximate expression.

Recent studies have been concerned with finding more details about cavity formation and appearance. Ding *et al.*[12] investigated the contact-line pinning during the impact of spheres by using a combination of theoretical analysis, simulations, and experiments; Marston *et al.*[13] focused on the crown splash generated by the impact of spheres, and carried out a detailed study on the buckling instability of the splash.

When a drop of liquid comes into contact with a hot solid, an evaporative vapor film can be formed between the drop and the solid surface if the surface temperature is significantly higher than the liquid's boiling point. The drop can levitate on the vapor film, which is called the Leidenfrost phenomenon first reported by Leidenfrost.[14] The lowest temperature of the solid surface is called the Leidenfrost temperature. The liquid drop can be sustained for a long time due to the low thermal conductivity of the vapor layer in this Leidenfrost regime, which can also be called the film-boiling regime. When the temperature of the surface drops below the Leidenfrost temperature, the system enters into the nucleate-boiling regime, the vapor layer collapses, and the drop boils immediately.

The boiling and heat transfer characteristics in nucleate-boiling and film-boiling regimes have been investigated by immersing a heated solid sphere into a liquid, observing the cooling process, and measuring the temperature of the sphere through using an inserted thermocouple-probe thermometer.[15–19] In the film-boiling regime, the sphere can be coated by a continuous vapor layer, preventing it from directly contacting the surrounding liquid. The stable vapor layer cannot be easily formed in low temperature water, as

*Project supported by the National Natural Science Foundation of China (Grant No. 11672094).

†Corresponding author. E-mail: weiyingjie@gmail.com

© 2018 Chinese Physical Society and IOP Publishing Ltd

reported by Yagov *et al.*[18] They argued that at high water subcoolings, film boiling exists in a particular boiling regime, which has been demonstrated through extensive experimental studies.[15,20] In this regime, the film is disturbed, and the heat transfer intensity is much higher than that for saturated film boiling.

Gylys *et al.*[21] and Vakarelski *et al.*[22] presented that the Leidenfrost effect can be used to reduce the drag of the sphere falling in a liquid. Vakarelski *et al.*[22] argued that the presence of the vapor layer can make the flow separation point move to the rear hemisphere, leading to the reduction of pressure drag which accounts for most of the total drag in their study. Zvirin *et al.*[20] investigated the drag and heat transfer characteristics of heated spheres free-falling in saturated and subcooled water after the impacts. Kenning[15] investigated the forced convective boiling around the spheres after the impacts at fixed velocities. They obtained various boiling form pictures for different impact velocities, water temperatures, and initial sphere temperatures. The studies of Zvirin *et al.*[20] and Kenning[15] showed that the cavities formed by these impacts of the spheres are not considered. Actually, the presence of cavities will influence the heat transfer properties due to the difference in thermal conductivity between liquid and air. The pressure distribution of the sphere will be changed when a cavity is formed, thus leading to the change of resistance. So, it is of great significance to investigate the temperature effects on cavity formation by the impact of a heated sphere.

Marston *et al.*[23] and Mansoor *et al.*[24] investigated the cavity formation by the impacts of heated spheres onto a fully fluorinated liquid, perfluorohexane, which has a low latent heat of vaporization and a low boiling point. In this liquid, a stable vapor layer can be formed at low sphere temperatures even at high subcoolings. This has also been demonstrated by Vakarelski *et al.*[22] and Yagov *et al.*[17] who used similar liquids. The particular film-boiling regime with high heat transfer intensity found in high subcooled water was not observed in perfluorohexane reported by Yagov *et al.*[17] The different boiling modes and heat transfer intensity may influence the impact characteristics, and there is no detailed investigation about the temperature effect on the cavity formation in the whole boiling regime.

In the present article, we present the detailed experimental results of a systematic investigation on cavity formation when heated spheres impact onto water at both low and high subcoolings. The impact characteristics are more complicated than those in our previous study,[25] in which we only had a preliminary investigation on cavity formation of heated spheres impact onto cold water (17 °C). In the present article, we investigate the sphere temperature effect on the cavity formation in both nucleate-boiling and film-boiling regimes for various impact velocities, water subcoolings, and initial temperatures of the sphere. We map the cavity regimes in the whole boiling regime. We specifically discuss the cavity instability in the film-boiling regime, in which the vapor layer around the sphere is disturbed or unstable.

2. Experimental setup

A schematic of our experimental apparatus is presented in Fig. 1. The spheres used were polished GCr15 bearing steel, with density $\rho_s = 7810$ kg/m^3, radius $R_0 = 10$ mm, and roughness $R_a < 0.06$ μm given by the manufacturer. The spheres were washed by alcohol and water to eliminate surface contamination. The water tank with inner dimensions 30 cm×30 cm×60 cm was made of tempered glass and heat-resistant glass sealant. A heat-resistant cushion was placed at the bottom of the water tank to prevent the bottom glass from being damaged due to the impact and high temperature of the spheres. The depth of the water was kept at 50 cm during the experiments.

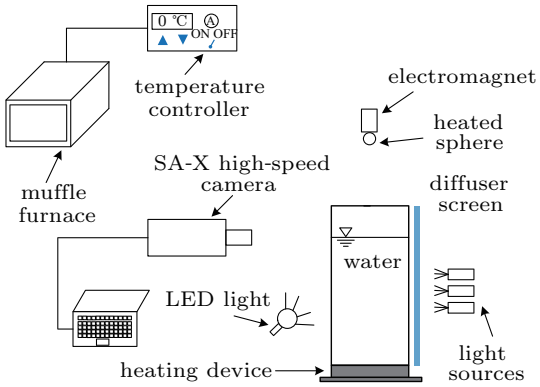


Fig. 1. (color online) Schematic diagram of experimental apparatus.

The water was heated by a heating device and stirred with a stirring rod to obtain a uniform water temperature. The spheres were heated to the required temperature and maintained for more than 40 min in a muffle furnace. The spheres were taken out and released by an electromagnet immediately when the water temperature reached the experimental value. The initial temperature of the spheres T_s varied from 30 °C to 500 °C, and the room temperature was 30 ± 2 °C during the experiments; the water temperatures in our experiments were $T_w = 30$ °C and 60 °C for high subcooled water and $T_w = 95$ °C for low subcooled water.

A high-speed camera (Photron Fastcam SA-X) was used to record the whole impact sequence at a frame rate of 5000 frames per second. Uniform back lighting was achieved by a group of 6 × 500 W light sources illuminating a diffuser screen. A foreground LED light was used in some experiments to observe the flow conditions on the sphere surface.

A variety of impact velocities were obtained by changing the releasing height of the spheres, and the exact speed of im-

pact, 1.2 m/s$\leq V_0 \leq$ 5.6 m/s, was determined directly from the video clips. The 30 °C, 60 °C, and 95 °C water have density $\rho = 995.6$ kg/m^3, 983.2 kg/m^3, and 961.9 kg/m^3, dynamic viscosity $\mu = 0.8$ mPa·s, 0.47 mPa·s, and 0.3 mPa·s, and water-air surface tension $\sigma = 71.2$ mN/m, 66.2 mN/m, 58 mN/m, respectively. The impact of the spheres is characterized by three non-dimensional numbers: Froude number $Fr = V_0^2/gR_0$ (where g is the gravitational acceleration), Reynolds number $Re = -\rho V_0 R_0/\mu$, and Weber number $We = \rho V_0^2 R_0/\sigma$. These non-dimensional numbers in our experiments were in the ranges $14.7 \leq Fr \leq 320$, $14934 \leq Re \leq 179555$, and $201 \leq We \leq 5201$.

3. Results and discussion

3.1. Threshold speed of cavity formation

In Fig. 2, we present impacts of a room-temperature sphere ($T_s = 30$ °C) and a heated sphere ($T_s = 200$ °C) onto water ($T_w = 30$ °C) at impact velocity $V_0 = 1.2$ m/s. We observe that the cavity only exists in the heated sphere case.

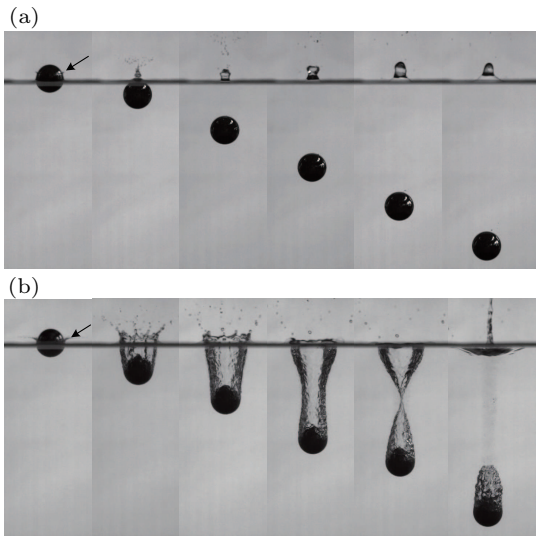


Fig. 2. Comparison of impacts of spheres onto water at $V_0 = 1.2$ m/s: (a) $T_s = 30$ °C, at time $t = 5$, 13.2, 30.2, 47.2, 64.4, 81.6 ms from impact; (b) $T_s = 200$ °C, at time $t = 5$, 19, 33, 51, 60.8, 81.6 ms from impact. In both cases, the water temperature is $T_w = 30$ °C.

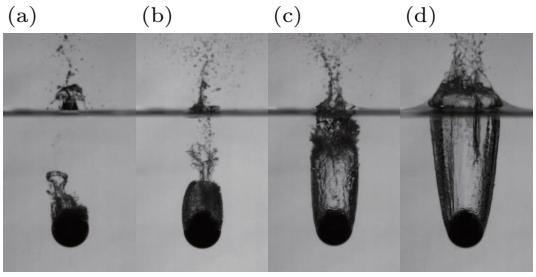


Fig. 3. Cavities at depth $H = 7R_0$ formed during impacts of spheres with $T_s = 30$ °C, $T_w = 30$ °C, $V_0 =$ (a) 4.2 m/s, (b) 4.5 m/s, (c) 5 m/s, and (d) 5.6 m/s.

For the room-temperature sphere, a cavity can be formed at larger impact velocities ($V_0 > 4.2$ m/s) as shown in Fig. 3. The features of the impacts are as follows: (a) small entrained air pocket; (b) small cavity; (c) partial cavity; and (d) full cavity. We consider the impact in Fig. 3(a) as the no cavity condition in the following description.

The cavity formation is related to the movement of the thin liquid film from the water (marked by the arrow in the first frame for both cases). In Fig. 2(a), the thin liquid film wraps around the sphere and adheres to the surface until closing at the apex. The sphere is surrounded by water and no cavity is formed. In Fig. 2(b), the thin liquid film is detached from the sphere surface after the impact, and a cavity is formed behind the sphere.

As shown by Duclaux *et al.*,[10] the cavity can be formed only when the impact velocity is above a threshold value. We can conclude that the threshold velocity for the heated sphere ($T_s = 200$ °C) is far less than that for the room-temperature sphere.

We observe another cavity formation at low impact speed ($V_0 = 1.2$ m/s) as shown in Fig. 4. The water temperature is $T_w = 95$ °C, and the initial sphere temperature is $T_s = 500$ °C. The mist is formed above the water surface when the water temperature is close to the boiling point. The characteristics of cavity walls in Figs. 2(b) and 4 are different (coarse in Fig. 2(b) and smooth with regular ripples in Fig. 4).



Fig. 4. Cavities formed during the impact of a sphere at $V_0 = 1.2$ m/s with $T_s = 500$ °C, $T_w = 95$ °C at time $t = 24.6$, 42.6, and 68.4 ms from impact.

The threshold velocity for room temperature spheres depends on the surface state and the liquid characteristic. The surface state may be changed after heating the sphere to a high temperature, and this might lead to the low threshold velocity for cases shown in Figs. 2(b) and 4. We heat a sphere to a temperature of 500 °C then cool the sphere to room temperature. We find that the cavity cannot be formed below the impact velocity of 4 m/s. The temperatures of our experimental spheres do not exceed the temperature of 500 °C. So the change of sphere surface states has little influence on the low threshold velocity.

As shown by Duez *et al.*,[9] the threshold velocity is proportional to the capillary velocity, defined as σ/μ. The water–air surface tension σ and the water dynamic viscosity μ decrease as the water temperature increases, and μ decreases at a larger rate, which leads to the increase of the capillary velocity. Thus, the threshold velocity for room temperature spheres will be high for high temperature water. We carry out experiments on the impacts of room-temperature spheres onto 60 °C and 95 °C water. We find that the cavity cannot be formed below the impact velocity of 4 m/s. So, the changes of water characteristics are not associated with the low threshold velocity.

Since the low threshold velocity cannot be due to the change of surface state and water characteristic, we suspect that it is a consequence of vaporization of water on the surface of the spheres. We present the surface vaporization states: Fig. 5(b), a case shown by Fig. 2(b); Fig. 5(c), a case shown by Fig. 4. We find that the surface flows are dissimilar to those of the room-temperature sphere shown in Fig. 5(a).

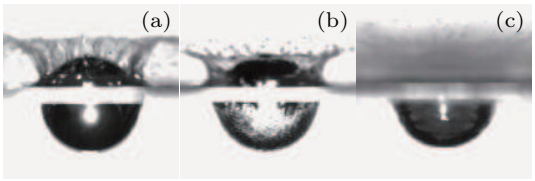


Fig. 5. Close-up cavity images at depth $H = R_0$, and (a) $V_0 = 5.6$ m/s, $T_w = 30$ °C, and $T_s = 30$ °C; (b) $V_0 = 1.2$ m/s, $T_w = 30$ °C, and $T_s = 200$ °C, a case shown by Fig. 2(b); (c) $V_0 = 1.2$ m/s, $T_w = 95$ °C, and $T_s = 500$ °C, a case shown by Fig. 4.

When a sphere with moderate temperature is immersed into water, nucleate boiling will occur around the sphere.[15] We also observe vapor bubbles generated by nucleate boiling on the surface, as shown in Fig. 5(b).

A coarse sphere has a low threshold velocity compared with a smooth sphere.[5] Both the coarseness of the sphere surface and the disturbance of the vapor bubbles can enhance the turbulence of the flow. Both coarse spheres and heated spheres with moderate temperatures can form cavities with rough walls. The rough cavities can also be formed at low velocities by impacting the spheres coated with viscous liquids due to the surface disturbance of the liquid layers reported by Bell[26] and May.[7] We suspect that the low threshold velocity shown in Fig. 2(a) is due to the disturbance of the vapor bubbles.

When a sphere with a high temperature (far above the boiling temperature) is immersed into water at low subcooling, film boiling occurs and a continuous vapor layer can be formed around the sphere.[15] This vapor layer is also observed in Fig. 5(c), and the sphere inside the vapor layer looks smaller than the sphere shown in Fig. 5(a) due to the refraction of light through different media (water and vapor). The regular ripples shown in Fig. 4 are caused by the repeated compression of the vapor layer when the sphere moves downward in the water.

A drop of water hitting a solid surface may bounce, provided that the surface is highly hydrophobic. As a similar situation, when the drop hits a very hot solid, a thin layer of vapor will be generated between the drop and the solid and may make the drop rebound.[27] We suspect that the vapor layer may have some similar properties to those of hydrophobic materials. From Fig. 1(a) taken by Quéré,[28] we find that the contact angle between the small water drop and the 300 °C metallic plate is more than 160°.

A cavity can be formed at a low impact velocity for a hydrophobic sphere relative to a hydrophilic sphere.[9,10] We compare the impact of a superhydrophobic sphere onto 30 °C water (Fig. 6(a)) with the impact of a heated sphere with an initial temperature of 400 °C onto 95 °C water (Fig. 6(b)), in which case a stable vapor layer can be generated around the sphere. The impact velocities in the above cases are both $V_0 = 1.2$ m/s.



Fig. 6. Comparison of impact between (a) a superhydrophobic sphere ($T_s = 30$ °C, $T_w = 30$ °C) and (b) a heated sphere ($T_s = 400$ °C, $T_w = 95$ °C) onto water at time $t = 6$, 23.6, 43, 53.6, 67.2, and 72.2 ms from impact, with an advance contact angle of about 170° and receding contact angle close to 160°. The impact velocities are both $V_0 = 1.2$ m/s.

The superhydrophobic sphere is prepared by using the methods given by Vakarelski *et al.*[16] with a commercially available coating agent (Glaco Mirror Coat Zero, Soft 99 Co.). The advance contact angle is about 170° and the receding contact angle is close to 160°.

The thickness of vapor layer increases as the temperatures of the sphere and water increase.[29] The initial temperature of the sphere shown in Fig. 6(b) is 400 °C which is lower than 500 °C for the case shown in Fig. 4. So the vapor layer is thinner in Fig. 6(b) and cannot be easily seen by eye. As a result, we cannot find the regular ripples shown in Fig. 4. However, this is really in the film-boiling regime, and we will discuss the boiling regimes for the impacts by heated spheres onto 95 °C water in Subsection 3.2.

The cavity appearances for the two impact processes shown in Fig. 6 are very similar, and in both cases the cav-

ity interfaces are smooth. The contact line emanates approximately from the equator of the superhydrophobic sphere as seen in Fig. 6(a), while the contact line is absent for the Leidenfrost impact shown in Fig. 6(b) due to the encapsulation of a thin vapor layer. We suspect that the vapor layer has a similar effect to the superhydrophobic sphere, which leads to the low threshold velocity for the cases shown in Figs. 4 and 6(b).

3.2. Stability of vapor layer

In Fig. 7, we present cavities at $H = 6R_0$ formed during impacts of spheres with different impact velocities and initial temperatures onto 95 °C water. As shown in Fig. 7(a), a cavity with rough interface is formed, which is similar to the cavity by the impact of a 200 °C sphere onto 30 °C water as shown in Fig. 2(b). In the nucleate-boiling regime, the heat transfer intensity is enhanced with the water and sphere temperature increasing. Large vapor bubbles can be seen around the sphere shown in Fig. 7(a).

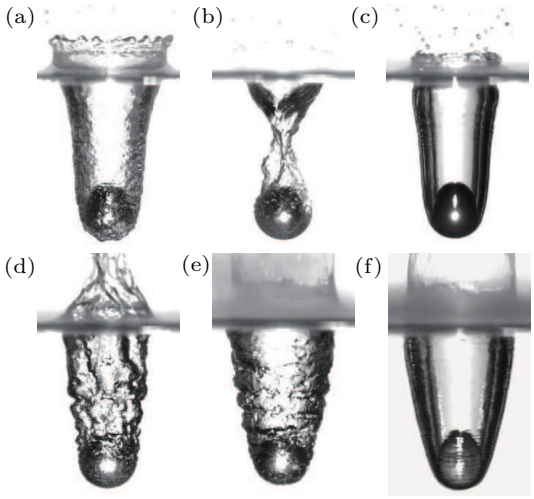


Fig. 7. Cavities formed at depth $H = 6R_0$ during impacts of spheres onto 95 °C water for (a) $T_s = 250$ °C and $V_0 = 1.2$ m/s, (b) $T_s = 300$ °C and $V_0 = 1.2$ m/s, (c) $T_s = 350$ °C and $V_0 = 1.2$ m/s, (d) $T_s = 350$ °C and $V_0 = 3.4$ m/s, (e) $T_s = 400$ °C and $V_0 = 5.6$ m/s, and (f) $T_s = 500$ °C and $V_0 = 5.6$ m/s.

With the increase of the sphere's initial temperature, vapor bubbles begin to gather together, leading to the transition from nucleate boiling to film boiling. When the sphere's initial temperature reaches to 300 °C, film boiling occurs and a vapor layer is formed on the surface of the sphere. The boiling intensity weakens due to the low thermal conductivity of vapor, and only a few small bubbles can be seen around the vapor layer. As the sphere temperature is not high enough, the vapor layer is unsteady. We cannot fully understand why the unsteady vapor layer leads to a cavity not fully developed as shown in Fig. 7(b). When the sphere's initial temperature reaches to 350 °C, the vapor layer becomes stable, producing a very smooth cavity as shown in Fig. 7(c) similar to the case shown in Fig. 6(b). There are no obvious bubbles around the vapor layer due to the continuous decrease of heat transfer intensity.

A drop may rebound when hitting a heated surface if the vapor (generated by vaporization) pressure overcomes the drop's dynamic pressure. The dynamic pressure of the drop is determined by *We* and the increase of the surface temperature can raise the vapor pressure. Thus the Leidenfrost temperature will increase with *We* increasing.[28,30,31] So the Leidenfrost temperature rises with the velocity increase of the drop for a specific liquid. Vakarelski *et al.*[29] also presented that the Leidenfrost temperature for a sphere falling through water is higher than that for a static sphere. They argued that the shear stresses induced on the vapor layer may cause the vapor layer to be unstable. In our experiments, we find a similar phenomenon: the destabilization of the vapor layer leads to an unstable cavity formed by the impact of a 350 °C sphere when increasing the impact velocity to 3.4 m/s, as shown in Fig. 7(d). We also find the disturbed cavity for a 400 °C sphere at an impact velocity of 5.6 m/s, as shown in Fig. 7(e). A stable vapor layer requires a high temperature of sphere at a high impact velocity. As shown in Fig. 7(f), when the initial temperature of the sphere is 500 °C, a stable vapor layer can be formed around the sphere, which leads to a smooth cavity with regular ripples at the impact velocity of 5.6 m/s.

In Fig. 8, we present the cooling progress of a 400 °C sphere held by the electromagnet still in 60 °C water. A stable vapor layer is formed on the surface after the sphere has been immersed into water. The vapor layer lasts about 30 s due to the low heat transfer intensity of film boiling. When the sphere temperature drops below the Leidenfrost temperature, vapor explosion occurs, then film boiling transfers to nucleate boiling with an explosive release of bubbles around the sphere.

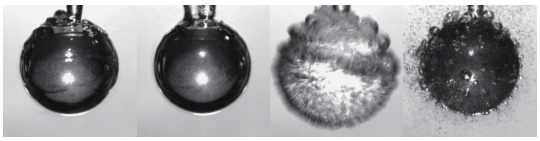


Fig. 8. Cooling process of a 400 °C sphere in 60 °C water at time $t = 1.84$, 30.07, 30.08, and 30.35 s after the sphere has immersed into water.

In Fig. 9(a), the stable vapor layer cannot be formed by the impact of the 400 °C sphere onto water at $V_0 = 1.2$ m/s. A shell of vapor around the sphere grows and collapses radially as shown in the supplementary movie. There is only small entrained air, and no cavity is formed. In Fig. 9(b), when the initial temperature of the sphere is 500 °C, a vapor layer is formed in the initial stage of the impact. The appearance of the vapor layer is different from the stable vapor layer formed during the impact of a 500 °C sphere onto 95 °C water shown in Fig. 4. We can see the micro bubbles around the vapor layer in the first two frames of Fig. 9(b), and hardly any of

the bubbles can be seen around the smooth and stable vapor layer shown in Fig. 4. The micro-bubble boiling has been considered as a particular film-boiling model for high subcooled water.[18,20] The stability of the vapor layer cannot be maintained for a long time due to the high heat transfer intensity in this boiling regime. The vapor layer around the sphere grows and collapses after several milliseconds, which is similar to the case shown in Fig. 9(a). No cavity is formed in this impact process. In high subcooled water, stable film boiling cannot easily occur, and in our impact experiments the stable vapor layer is not observed for $T_w = 30$ °C and $T_w = 60$ °C.

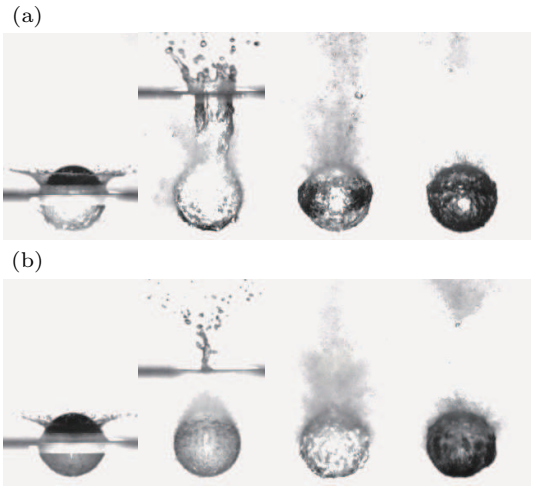


Fig. 9. Impacts of heated spheres onto 60 °C water at $V_0 = 1.2$ m/s for (a) $T_s = 400$ °C at time $t = 6.6$, 28.8, 50.6, and 81.6 ms after impact, and (b) $T_s = 500$ °C at time $t = 6.6$, 28.8, 50.6, and 81.6 ms after impact.

3.3. Irregular cavities

In our experiments, no cavities are formed by the impact of heated spheres with initial temperatures higher than 300 °C onto high subcooled water ($T_w = 30$ °C, $T_w = 60$ °C) at an impact velocity of 1.2 m/s. When increasing the impact velocity, in some cases, cavities are formed due to the influence of the velocity. However, none of the cavities can be fully developed and will break into fragments. In Fig. 10, we show some broken cavities for different impact velocities and initial sphere temperatures.

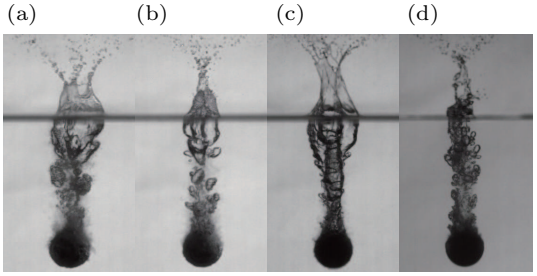


Fig. 10. Broken cavities at depth $H = 8R_0$ for (a) $T_w = 30$ °C, $T_s = 350$ °C, and $V_0 = 5.6$ m/s, (b) $T_w = 30$ °C, $T_s = 450$ °C, and $V_0 = 3.4$ m/s, (c) $T_w = 60$ °C, $T_s = 400$ °C and $V_0 = 3.4$ m/s, and (d) $T_w = 60$ °C, $T_s = 450$ °C, and $V_0 = 5.6$ m/s.

The nucleate-boiling and film-boiling regimes in the cooling progress are usually distinguished by the heat transfer intensity determined with the temperature of the sphere measured by an embedded thermal couple.[16–18] The heat transfer intensity of nucleate boiling is usually an order of magnitude higher than that of film boiling. While high heat transfer intensity is also found for spheres whose temperature is far above the critical temperature of water.[20] According to the classic theory of homogeneous nucleation, under these conditions the liquid–vapor phase transition occurs practically instantly, where the characteristic time is on the order of ns. The nucleate boiling cannot occur under such conditions reported by Yagov *et al.*[18] and it is referred to as a particular mode of film boiling. The low heat transfer intensity exists only in stable film-boiling regime with a stable vapor layer around the sphere. There is no stable film-boiling regime for $T_w = 30$ °C and $T_w = 60$ °C by the impact of heated spheres in our experiments. When the temperature of the sphere is above 300 °C, vapor fragments or an unstable vapor layer may be formed on the surface. The broken cavities may be due to the high heat transfer intensity and the disturbance of the vapor layer or vapor fragments.

Figure 11 shows the dual cavities similar to those shown in Fig. 13 from Marston *et al.*[23] In our experiments, the dual cavities can be formed for the cases of nucleate boiling (Figs. 11(a) and 11(b)) and film boiling (Fig. 11(c)). The ranges of the impact velocities and the initial sphere temperatures in which dual cavities can be formed for the three water temperatures are shown in Fig. 13.

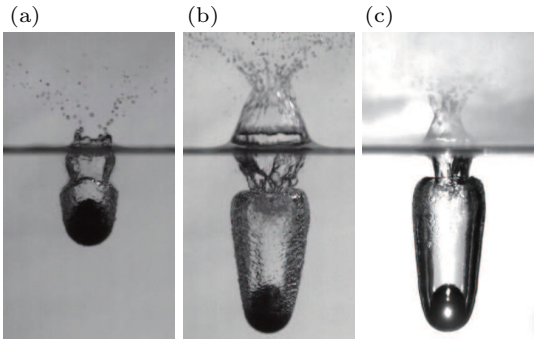


Fig. 11. Dual cavities formed during the impacts for (a) $T_w = 30$ °C, $T_s = 260$ °C, and $V_0 = 1.2$ m/s, (b) $T_w = 30$ °C, $T_s = 280$ °C, and $V_0 = 2.5$ m/s, and (c) $T_w = 95$ °C, $T_s = 350$ °C, and $V_0 = 4.5$ m/s.

In Fig. 12, we present the evolutionary process of a dual cavity for the nucleate boiling case. The water temperature is $T_w = 30$ °C, the initial sphere temperature is $T_s = 280$ °C, and the impact velocity is $V_0 = 5.6$ m/s. As shown in Fig. 12(a), before the formation of the dual cavity, a number of bubbles attach to the bottom hemisphere, the cavity-sphere contact line (marked by the arrow) is located at the top hemisphere surface. When the dual cavity is formed, as shown in Fig. 12(b), there are hardly any bubbles around the bottom hemisphere and the cavity-sphere contact line is located at the sphere equator. The bubbles around the bottom hemisphere are merged with the

upper cavity due to the low pressure at the sphere equator, and the contact line moves downward, leading to a new cavity structure. Thereafter, the contact line is pinned at the sphere equator, as shown in Figs. 12(c) and 12(d). The top and bottom cavities are connected, air passes through the top cavity and enters into the bottom cavity till the surface seals.

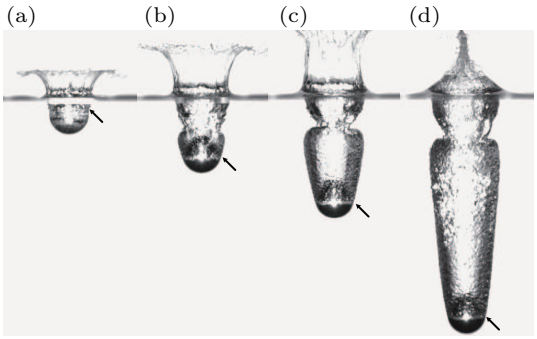


Fig. 12. Evolutionary process of a dual cavity by the impact of a sphere for $T_w = 30$ °C, $T_s = 280$ °C, $V = 5.6$ m/s, at time $t = 3.2$, 7, 11.6, and 23.4 ms from impact.

The dual cavity formed in the film-boiling regime is similar to that in the nucleate boiling regime. The vapor is disturbed by the impact with bubbles around it before the formation of the dual cavity, and the location of the contact line is also at the top hemisphere surface. Then the vapor layer becomes stable and a very smooth dual cavity can be formed. The bottom hemisphere is covered by the vapor layer, no contact line can be found for this case, as shown in Fig. 11(c). So, the formation of the dual cavity for both cases needs a large change of the flow states at the sphere surface, and the contact line must be located at the top hemisphere surface at the beginning of the impact.

3.4. Summary of observations in V_0–T_s space

The transitions between different cavity features shown in the previous sections are summarized in Fig. 13. We also consider the small entrained air pocket shown in Fig. 3(a) as the no cavity case. The impacts shown in Figs. 3(b), 3(c), and 7(b), in which the cavities cannot be fully developed, are considered as the incomplete cavity cases.

The distribution characteristics of impact features for 95 °C water are different from those for 30 °C and 60 °C water due to the different heat transfer and boiling characteristics for high subcooled and low subcooled water. The distribution characteristics of cavity properties are similar for 30 °C and 60 °C water, and from Fig. 13(a) to Fig. 13(b) the data points seem to move left.

Like cold spheres, when the vaporization effect is not obvious in the film-boiling regime, cavities can only be formed at high impact velocities (see the data points in the first columns for these three different water temperatures). The minimum initial temperature of the sphere for a full cavity at an impact velocity of 1.2 m/s decreases with the increase of water temperature. As described in Subsection 3.1, the cavities formed by the impacts of spheres with moderate initial temperatures are due to the disturbance of the vaporized bubbles around the spheres. In high temperature water, more bubbles can be formed, which leads to the disturbance being enhanced (e.g., Fig. 7(a)).

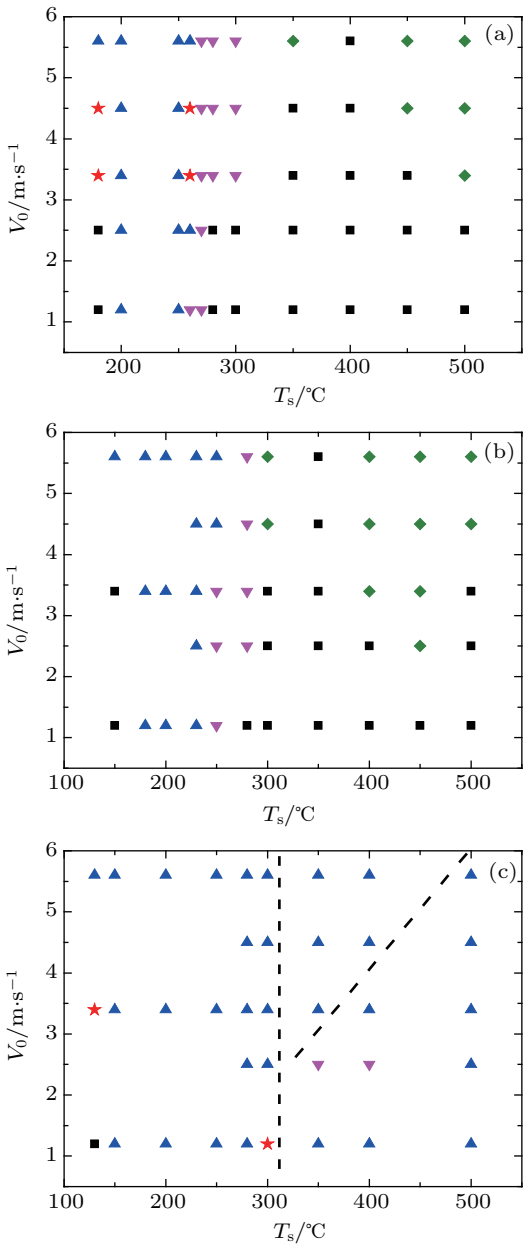


Fig. 13. (color online) Maps of V_0–T_s parameter space, showing transitions between cavity features for different water temperatures: (a) $T_w = 30$ °C, (b) $T_w = 60$ °C, and (c) $T_w = 95$ °C. The vertical dashed line in panel (c) indicates temperature beyond which a stable vapor layer can be formed around the sphere at low impact velocities. The inclined dashed line indicates the transition from smooth cavity (bottom) to disturbed cavity (top). The impact features are classified as no cavity (■), incomplete cavity (⋆), full cavity (▲), dual cavity (▼), and broken cavity (⧫).

Dual cavities can only be formed in a small temperature range for all water temperatures. For $T_w = 30$ °C and 60 °C,

the temperature range is between 250 °C and 300 °C in the nucleate boiling regimes. The dual cavities are found to be formed at low impact velocities for low sphere temperatures and at high impact velocities for high sphere temperatures. For $T_w = 95$ °C, the dual cavity is formed under the condition of film boiling when the initial temperatures of the spheres are above 300 °C.

For 95 °C water, the full cavities are formed in the whole range of initial sphere temperatures. The cavity formed at an impact velocity of 1.2 m/s for $T_s = 300$ °C is incomplete, and the heat transfer is in the transition stage between nucleate boiling and film boiling. Smooth cavities can be formed when the initial sphere temperatures are beyond 300 °C at low impact velocities (e.g., Figs. 4, 6(b), and 7(c)). The vapor layers formed around the spheres can be disturbed by high impact velocities, thus resulting in disturbed cavities (see the data points beyond the inclined dashed line in Fig. 13(c)) (e.g., Figs. 7(d) and 7(e)). By increasing the initial sphere temperature, the smooth cavities can be formed at higher impact velocities (e.g., Fig. 7(f)). Stable vapor layers are not easy to form at high subcooled water, so we only find broken cavities beyond the temperature of 300 °C for 30 °C and 60 °C water due to the high heat transfer intensity.

3.5. Pinch-off time

Pinch-off (deep closure) is an important characteristic for cavity dynamics. The high-speed camera is set to have a small field of vision to obtain the highresolution snapshots. So, we can obtain none of the positions of the spheres when pinch-off occurs at high impact velocity. Here, we just investigate the pinch-off time, τ, when pinch-off occurs at one point, hence we can obtain the precise values. In accordance with Duclaux *et al.*,[10] the pinch-off time is nearly independent of the impact velocity for our experiments, so we use the same symbols for different impact velocities with the same temperature of spheres and water.

The pitch-off time is nearly independent of both the initial sphere temperature and the water temperature, as shown in Fig. 14. Our best fit to this time yields $\tau \approx 67$ ms. Duclaux *et al.*[10] found the pitch-off time $\tau \approx k\sqrt{R_0/g}$ with a prefactor $k = 2.06$ for a hydrophobic sphere. In our experiments we find the prefactor $k = 2.1$. Marston *et al.*[23] found $k = 2.09$ for heated spheres impacting onto a fluorinated liquid. There are very small differences between these three prefactor values, so the pitch-off characteristics are similar for these experiments.

The initial radius of cavity expansion is equal to the sphere radius when the contact line is located at the sphere equator. For most cases, the contact line is pinned at the sphere equator after the impact, as in most cases in our experiments. So the sphere radius R_0 is usually used to represent the initial cavity radius in the expression, $\sqrt{R_0/g}$. The prefactor value k is related to the initial expansion speed of the cavity, as described by Duclaux *et al.*[10] The contact lines for low initial sphere temperatures for $T_w = 30$ °C and 60 °C are slightly above the equator of the sphere due to the low disturbance intensity, as shown in Fig. 2(b), thus the initial cavity radius is smaller than R_0, which also leads to the low initial expansion speed of the cavity, so the pinch-off time has relatively low values for these cases (see the data points inside the dashed ellipse).

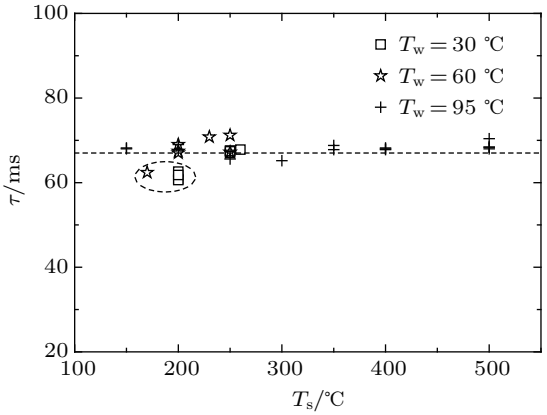


Fig. 14. Pinch-off time versus initial sphere temperature for $T_w = 30$ °C (□), 60 °C (☆), and 95 °C (+). The dashed line indicates the mean value from the data sets.

4. Conclusions

We have summarized observations from an experimental study on cavity formation during water entry of heated spheres. The results show how the temperature of the sphere affects the cavity formation for both low and high subcooled water. In the nucleate-boiling regime, we observe a rough cavity formed at a very low impact velocity. At the same impact velocity, a very smooth cavity can be formed in the film-boiling regime with a stable vapor layer around the sphere for 95 °C water. It is most likely that the formation of the rough cavity is due to the disturbance of the vapor bubbles and the formation of the smooth cavity is due to the hydrophobic effect of the vapor layer. We compare the impacts of a cold superhydrophobic sphere and a heated sphere in the film-boiling regime, and find that their cavity appearances are extremely similar. The regular ripples on the cavity interface can be seen if the vapor layer has a large thickness. In high temperature water, large bubbles can be formed in the nucleate-boiling regime, which leads to violent disturbance. In this case, a rough cavity can be formed at low impact velocities with a relatively low initial sphere temperature.

We summarize our observations in V_0–T_s space for different water temperatures. The distribution characteristics of cavity features for 95 °C water are different from those for 30 °C and 60 °C water due to the differences in heat transfer and boiling characteristic between high subcooled and low subcooled

water. For low subcooled water (95 °C water), the full cavities can be formed in the whole range of initial sphere temperatures. The stable vapor layers formed around the spheres in the film-boiling regime can be disturbed by high impact velocities, which leads to disturbed cavities. When increasing the initial sphere temperature to a high value, the stable vapor layer and smooth cavity can also be formed at high impact velocities. For high subcooled water (30 °C and 60 °C water), neither the stable vapor layer nor the smooth cavity can be formed in our experiments. The film boiling has a particular model with high heat transfer intensity. In this case, no cavity can be formed at low impact velocity and only a broken cavity can be formed at high impact velocity.

At the beginning of some impacts in nucleate-boiling or film-boiling regimes, the cavity-sphere contact line is located at the top hemisphere surface and the bottom hemisphere surface is covered by a number of bubbles or a disturbed vapor layer with bubbles around it. The bubbles can be merged with the upper cavity, leading to the formation of a dual cavity.

The pitch-off time is nearly independent of both the initial sphere temperature and the water temperature in our experiments. We find pitch-off time $\tau \approx 2.1\sqrt{R_0/g}$, scaling as $\sqrt{R_0/g}$, which is consistent with previous studies. The contact lines by the impacts of spheres with low initial temperatures onto 30 °C and 60 °C water are slightly above the equator of the sphere, which leads to the relatively low pitch-off time.

References

[1] Seddon C M and Moatamedi M 2006 *Int. J. Impact Eng.* **32** 1045

[2] Von Kármán T 1929 *Tech. Report Archive & Image Library NACA TN* 321, Washington, USA

[3] May A 1952 *J. Appl. Phys.* **23** 1362

[4] Worthington A M 1908 *Longmans Green*

[5] Worthington A M and Cole R S 1897 *Phil. Trans. R. Soc. Lond. A* **189** 137

[6] Worthington A M and Cole R S 1900 *Phil. Trans. R. Soc. Lond. A* **194** 175

[7] May A 1951 *J. Appl. Phys.* **22** 1219

[8] Aristoff J M, Truscott T T, Techet A H and Bush J W M 2010 *Phys. Fluids* **22** 032102

[9] Duez C, Ybert C, Clanet C and Bocquet L 2007 *Nat. Phys.* **3** 180

[10] Duclaux V, Caillé F, Duez C, Ybert C, Bocquet L and Clanet C 2007 *J. Fluid Mech.* **591** 1

[11] Aristoff J M and Bush J W M 2009 *J. Fluid Mech.* **619** 45

[12] Ding H, Chen B Q, Liu H R, Zhang C Y, Gao P and Lu X Y 2015 *J. Fluid Mech.* **783** 504

[13] Marston J O, Truscott T T, Speirs N B, Mansoor M M and Thoroddsen S T 2016 *J. Fluid Mech.* **794** 506

[14] Leidenfrost J G 1966 *Int. Heat Mass Transf.* **9** 1153

[15] Kenning D B R 2004 *Int. J. Heat Fluid Flow* **25** 209

[16] Vakarelski I U, Patankar N A, Marston J O, Chan D Y C and Thoroddsen S T 2012 *Nature* **489** 274

[17] Yagov V V, Leksin M A, Zabirov A R and Denisov M A 2016 *Int. Heat Mass Transf.* **100** 918

[18] Yagov V V, Lexin M A, Zabirov A R and Kaban'kov O N 2016 *Int. Heat Mass Transf.* **100** 98

[19] Gylys J, Skvorcinskiene R, Paukstaitis L, Gylys M and Adomavicius A A 2016 *Int. Heat Mass Transf.* **95** 709

[20] Zvirin Y, Hewitt G R and Kenning D B R 1990 *Exp. Heat Transf.* **3** 185

[21] Gylys J, Skvorcinskiene R, Paukstaitis L, Gylys M and Adomavicius A A 2015 *Int. Heat Mass Transf.* **89** 913

[22] Vakarelski I U, Marston J O, Chan D Y C and Thoroddsen S T 2011 *Phys. Rev. Lett.* **106** 214501

[23] Marston J O, Vakarelski I U and Thoroddsen S T 2012 *J. Fluid Mech.* **699** 465

[24] Mansoor M M, Vakarelski I U, Marston J O, Mansoor M M and Thoroddsen S T 2017 *J. Fluid Mech.* **823** 716

[25] Li J C, Wei Y J, Wang C and Deng H Y 2016 *Acta Phys. Sin.* **65** 204703 (in Chinese)

[26] Bell G E 1924 *Phil. Mag.* **648** 75

[27] Biance A L, Chevy F, Clanet C, Lagubeau G and Quéré D 2006 *J. Fluid Mech.* **554** 47

[28] Quéré D 2013 *Annu. Rev. Fluid Mech.* **45** 197

[29] Vakarelski I U, Chan D Y C and Thoroddsen S T 2014 *Soft Matter* **10** 5662

[30] Bernardin J D and Mudawar I 2004 *J. Heat Transf.* **126** 272

[31] Tran T, Staat H J J, Prosperetti A, Sun, C and Lohse D 2012 *Phys. Rev. Lett.* **108** 036101